Robust MIMO LQR Control with Integral Action for Differential Drive Robots: A Lyapunov-Cost Function Approach

Anh-Minh Duc Tran
Modeling Evolutionary Algorithms Simulation and Artificial Intelligence, Faculty of Electrical and Electronics Engineering, Ton Duc Thang University, Ho Chi Minh City, Vietnam
tranducanhminh@tdtu.edu.vn (corresponding author)

Tri Vien Vu
Modeling Evolutionary Algorithms Simulation and Artificial Intelligence, Faculty of Electrical and Electronics Engineering, Ton Duc Thang University, Ho Chi Minh City, Vietnam
vutrivien@tdtu.edu.vn

Received: 18 April 2025 | Revised: 27 May 2025 | Accepted: 1 June 2025

 DOI: https://doi.org/10.48084/etasr.11583

ABSTRACT

This study introduces an LQR-enhanced MIMO state feedback system with integral action to ensure precise trajectory tracking by eliminating persistent offsets. Unlike standard LQR methods, the proposed approach integrates integral action without requiring separate disturbance observers, reducing computational complexity for embedded systems. A unique Lyapunov-based analysis, leveraging the LQR cost function, confirms stability with uniform ultimate boundedness despite external perturbations. MATLAB simulations reveal RRMSE values under 10% for longitudinal speed and yaw rate, even when subjected to step and stochastic disturbances. This method outperforms conventional PID and LQR-feedforward techniques, offering a lightweight, efficient solution for DDWMR applications in industrial logistics, field exploration, and real-time robotic systems.

Keywords-MIMO control; differential drive wheeled mobile robot; LQR; integral action; Lyapunov stability

I. INTRODUCTION

A. Background

Differential Drive Wheeled Mobile Robots (DDWMRs) are valued for their mechanical simplicity and maneuverability, featuring two independently driven wheels and a passive caster for stability, enabling precise control of longitudinal speed (v) and yaw rate (ω) for tasks like zero-radius turns and trajectory tracking in constrained environments. Widely used in industrial logistics, service robotics, and outdoor exploration [1, 2], DDWMRs face control challenges as a Multi-Input Multi-Output (MIMO) system due to the coupling of v and ω, compounded by external disturbances such as uneven terrain or payload shifts. The foundational kinematic and dynamic models in [1] and [2] guide research, while recent advances in machine learning for adaptive control [3], reinforcement learning for unstructured environments [4], robust optimization for agriculture [5], and LQR-MPC strategies for precise path tracking [6] highlight the need for robust, efficient control solutions.

B. Problem Statement

Controlling DDWMRs is a complex Multi-Input Multi-Output (MIMO) problem that requires precise regulation of v and ω amidst external disturbances, such as uneven terrain, wind forces, or payload shifts. Conventional PID controllers treat v and ω independently, leading to oscillations and steady-state errors under disturbances, as noted in [7]. Standard LQR approaches [8] account for coupled states but fail to eliminate persistent offsets from constant disturbances, such as inclinations, limiting tracking accuracy [9]. Advanced methods, including neural networks [3, 10], reinforcement learning [4, 11], and Model Predictive Control (MPC) [12, 13], provide robustness but demand significant computational resources, making them unsuitable for embedded systems. Robust control with disturbance observers [14], sliding mode control [15], or adaptive control [16-18] ensures stability but may introduce complexity, chattering, or transient instability. Robust frameworks [19, 20] and event-triggered strategies [21] address specific disturbances but lack generality. Lyapunov-based methods [22, 23] ensure stability but often oversimplify MIMO dynamics. This underscores the need for a lightweight and robust control strategy for accurate v and ω tracking and stability in diverse DDWMR applications.

C. Approach Overview

This study proposes an LQR-based MIMO state-feedback controller augmented with integral action to address these challenges. By incorporating integral action, the controller eliminates steady-state errors, a key limitation of standard LQR [8], without relying on a separate disturbance observer, as seen in some robust designs [24]. Unlike complex methods such as MPC or neural networks [3, 12, 25, 26], this approach offers a lightweight solution, ideal for resource-constrained embedded systems. Similar computational challenges of neural network-based methods are observed in robotic arm control and path planning [25, 26]. The LQR framework optimizes control effort across the coupled states, balancing performance and efficiency, while a novel Lyapunov stability analysis leverages the LQR cost function to prove uniform ultimate boundedness under bounded disturbances. This approach contrasts with neural networks, RL, and MPC by offering a lightweight yet robust solution, and advances beyond traditional Lyapunov methods by integrating optimality with stability analysis.

D. Summary of Main Findings

Extensive MATLAB simulations over a duration of 2.5 s demonstrate the controller's effectiveness. The RRMSE for v and ω remains below 10%, even under step and random disturbances. Stability is confirmed through negative eigenvalues of the closed-loop system and bounded Lyapunov trajectories. Compared to PID and standard LQR with feedforward, this method provides improved tracking accuracy and effective disturbance handling, positioning it as a practical solution for DDWMR applications.

II. SYSTEM MODEL

Effective control design for DDWMRs begins with a robust system model that encapsulates the robot's electromechanical dynamics, control inputs, measurable outputs, and external disturbances. The DDWMR is modeled as a MIMO system with a state vector $\mathrm{x} = [i_{aR}, \omega_R, i_{aL}, \omega_L]^T$, where i_{aR} and i_{aL} are the right and left motor currents, and ω_R and ω_L are the corresponding wheel angular velocities. Control inputs are defined as $\mathrm{u} = [V_{aR}, V_{aL}]^T$, representing the voltages applied to the right and left motors, respectively. The outputs of interest, $\mathrm{y} = [v, \omega]^T$, denote the robot's longitudinal speed and yaw rate, derived from wheel velocities via kinematic relationships. External disturbances, such as terrain-induced forces or payload torques, are captured by $\mathrm{d} = [F_D, T_D]^T$, where F_D is a disturbance force and T_D is a disturbance torque.

The system dynamics are expressed in state-space form:

$$\dot{\mathrm{x}} = \mathrm{Ax} + \mathrm{Bu} + \mathrm{B}_d\mathrm{d}, \quad \mathrm{y} = \mathrm{Cx}, \tag{1}$$

where the matrices are:

$$\mathrm{A} = \begin{bmatrix} -61.8667 & -38.1972 & 0 & 0 \\ 49.0604 & -0.9419 & -18.3173 & 0.3517 \\ 0 & 0 & -61.8667 & -38.1972 \\ -18.3173 & 0.3517 & 49.0604 & -0.9419 \end{bmatrix},$$

$$\mathrm{B} = \begin{bmatrix} 66.6667 & 0 \\ 0 & 0 \\ 0 & 66.6667 \\ 0 & 0 \end{bmatrix}, \mathbf{B}_d = \begin{bmatrix} 0 & 0 \\ -1.1836 & -12.9702 \\ 0 & 0 \\ -1.1836 & 12.9702 \end{bmatrix},$$

$$\mathrm{C} = \begin{bmatrix} 0 & 0.0187 & 0 & 0.0187 \\ 0 & 0.0937 & 0 & -0.0937 \end{bmatrix}$$

This model builds upon prior work [27], where a general state-space representation of DDWMRs was introduced with distinct parameters for the left and right motor-wheel systems to capture asymmetric characteristics. In contrast, this study assumes identical parameters for both sides, simplifying the model while retaining its MIMO structure. A key improvement over [27] is the incorporation of external disturbances F_D and T_D, represented through the disturbance input matrix B_d, which enhances the model's applicability to real-world scenarios involving terrain variations or payload shifts. The A matrix reflects the interplay of motor electrical dynamics and mechanical coupling between wheels, derived from physical parameters such as resistance, inductance, and viscous friction. The B matrix shows direct voltage influence on motor currents, while B_d captures the asymmetric impact of disturbances on wheel velocities due to the differential drive layout. The C matrix translates wheel velocities into v and ω tied to wheel radius and robot base width, consistent with kinematic models in [1, 2]. Figure 1 illustrates the robot's configuration, and Figure 2 provides a block diagram of the state-space model, highlighting signal flow from inputs and disturbances to outputs.

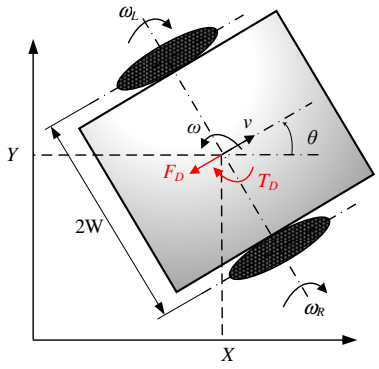

Fig. 1. Schematic diagram of a DDWMR.

This model comprehensively represents the DDWMR's behavior, serving as the foundation for controller design. Its fidelity to established modeling principles ensures its suitability for both theoretical analysis and practical implementation in real robotic systems.

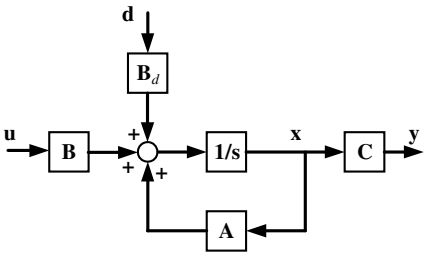

Fig. 2. Block diagram of the DDWMR state-space model.

III. CONTROLLER DESIGN AND STABILITY ANALYSIS

Designing a controller for DDWMRs requires addressing steady-state errors and ensuring robustness against disturbances such as terrain variations. This section presents an LQR-based MIMO state feedback controller with integral action, followed by a detailed stability analysis.

A. Controller Design

Here, an LQR-augmented MIMO feedback mechanism is designed with integral terms, addressing steady-state errors and ensuring robustness against disturbances such as terrain variations. The goal is to follow a desired path defined by $r = [v_{ref}, \omega_{ref}]^T$, producing outputs $y = [v, \omega]^T$. The tracking error is $e = r - y$, and integral action is introduced via $x_{int} = \int_0^t e(\tau)d\tau$, with dynamics $\dot{x}_{int} = e$. Augmenting the original state x with x_{int}, the state vector becomes $x_{aug} = [x^T, x_{int}^T]^T$, and the system dynamics are:

$$\dot{x}_{aug} = A_{aug}x_{aug} + B_{aug}u + B_d^{aug}d + E_{aug}r, \quad (2)$$

where:

$$A_{aug} = \begin{bmatrix} A & 0 \\ -C & 0 \end{bmatrix}, B_{aug} = \begin{bmatrix} B \\ 0 \end{bmatrix}, B_d^{aug} = \begin{bmatrix} B_d \\ 0 \end{bmatrix}, \text{and } E_{aug} = \begin{bmatrix} 0 \\ I \end{bmatrix}$$

are the augmented system matrices. Figure 3 depicts this structure, showing the feedback loop with integral action.

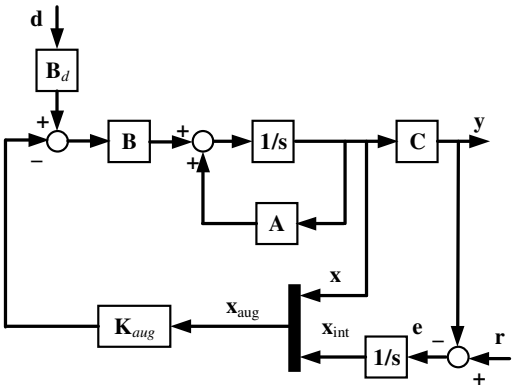

Fig. 3. Block diagram of the augmented control system with integral action.

For LQR design, consider the disturbance-free, reference-free case ($d = 0, r = 0$):

$$\dot{x}_{aug} = A_{aug}x_{aug} + B_{aug}u \quad (3)$$

The cost function to minimize is:

$$J = \int_0^\infty (x_{aug}^T Q x_{aug} + u^T R u)dt, \quad (4)$$

with $Q = \text{diag}([1{,}50, 1{,}50, 5 \times 10^7, 5 \times 10^6])$, emphasizing integral states for error elimination, and $R = I_2$. Solving the Algebraic Riccati Equation (ARE):

$$A_{aug}^T P_{aug} + P_{aug}A_{aug} - P_{aug}B_{aug}R^{-1}B_{aug}^T P_{aug} + Q = 0 \quad (5)$$

yields P_{aug}, and the feedback gain is $K_{aug} = R^{-1}B_{aug}^T P_{aug}$. The control law $u = -K_{aug}x_{aug}$ results in closed-loop dynamics:

$$\dot{x}_{aug} = (A_{aug} - B_{aug}K_{aug})x_{aug} + B_d^{aug}d \quad (6)$$

B. Stability Analysis

Stability under bounded disturbances ($\| d \| \leq d_{max}$) is assessed using a Lyapunov function $V = x_{aug}^T P_{aug} x_{aug}$, where P_{aug} from the ARE is positive definite. The time derivative is:

$$\dot{V} = x_{aug}^T (A_{cl}^T P_{aug} + P_{aug}A_{cl})x_{aug} + 2x_{aug}^T P_{aug} B_d^{aug} d \quad (7)$$

where $A_{cl} = A_{aug} - B_{aug}K_{aug}$. Using the ARE property:

$$A_{cl}^T P_{aug} + P_{aug}A_{cl} = -(Q + K_{aug}^T R K_{aug}) \quad (8)$$

(7) is simplified to:

$$\dot{V} = -x_{aug}^T (Q + K_{aug}^T R K_{aug})x_{aug} + 2x_{aug}^T P_{aug} B_d^{aug} d \quad (9)$$

The first term is negative definite, and bounding the disturbance term gives:

$$\dot{V} \leq -\lambda_{min} \| x_{aug} \|^2 + 2 \| P_{aug} B_d^{aug} \| \| x_{aug} \| d_{max} \quad (10)$$

where λ_{min} is the minimum eigenvalue of $Q + K_{aug}^T R K_{aug}$. For large $\| x_{aug} \|$, $\dot{V} < 0$, ensuring convergence to a bounded region proves uniform ultimate boundedness [28]. This aligns with Lyapunov-based analyses for autonomous mobile robots, where nonlinear dynamics are stabilized under bounded conditions [29]. Unlike observer-based methods [24], this approach relies on LQR and integral action for robustness, reducing complexity.

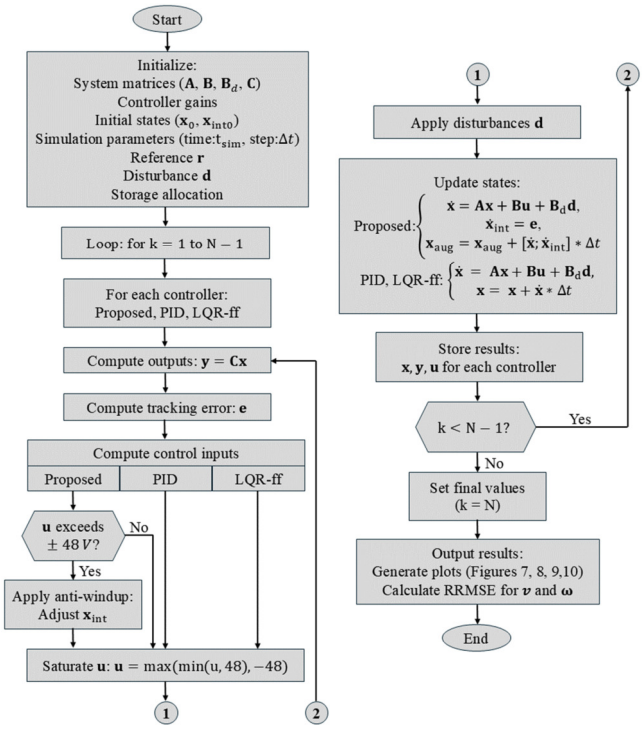

Fig. 4. Flowchart of the MATLAB simulation framework for the DDWMR control system.

IV. SIMULATION RESULTS

To evaluate the proposed MIMO LQR controller with integral action, MATLAB simulations were carried out over a 2.5-s duration, reflecting realistic DDWMR operating conditions. The simulations were carried out using a MATLAB script, implementing numerical integration of the DDWMR state-space model described in Section II, as illustrated in the simulation flowchart in Figure 4. The controller was compared against PID and LQR-feedforward (LQR-ff) baselines, selected for their widespread use and comparable complexity in embedded systems [7, 8]. Two disturbance scenarios, step and random, were examined to simulate challenges such as terrain changes or noise, assessing tracking accuracy, disturbance rejection, and computational efficiency.

A. Disturbance Scenarios

1) Step Disturbances

Step disturbances simulate abrupt external forces or torques, such as terrain variations or payload shifts. The profile, detailed in Figure 5, includes F_D and T_D variations over 0-2.5 s.

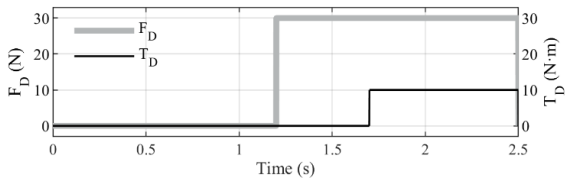

Fig. 5. Step disturbance profiles for force F_D (N) and torque T_D (N·m) applied to the DDWMR system over the simulation duration.

2) Random Disturbances

Random disturbances emulate stochastic disturbances such as uneven terrain or wind gusts, modeled as Gaussian noise with zero mean, standard deviations of 20 N for F_D and 5 N·m for T_D, and applied over 0-2.5 s. Noise values are segmented into 0.1 s intervals, with bounds of $[-30,30]$ N for F_D and $[-10,10]$ N·m for T_D. Figure 6 shows the profile.

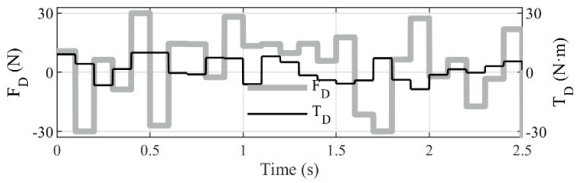

Fig. 6. Gaussian disturbance profiles for force F_D (N) and torque T_D (N·m) applied to the DDWMR system over the simulation duration.

B. Controller Structures for Comparison

To provide a comprehensive evaluation, the proposed LQR-based MIMO controller with integral action was benchmarked against two established methods: a traditional Proportional-Integral-Derivative (PID) controller and a standard Linear Quadratic Regulator with feedforward (LQR-ff). The structures of these baseline controllers, implemented as part of the simulation framework, are summarized based on their design and tuning for the DDWMR system.

1) PID Controller

The PID controller independently regulates the v and ω of the DDWMR, following the classical approach outlined in [7]. It employs separate PID loops for v and ω, with control inputs V_{aR} and V_{aL} calculated as combinations of these outputs. The control law is defined as:

$$\text{For } v\text{: } u_v = K_{p_v} e_v + K_{i_v} \int e_v dt + K_{d_v} \frac{de_v}{dt}$$

$$\text{For } \omega\text{: } u_\omega = K_{p_\omega} e_\omega + K_{i_\omega} \int e_\omega dt + K_{d_\omega} \frac{de_\omega}{dt}$$

where $e_v = v_{\text{ref}} - v$ and $e_\omega = \omega_{\text{ref}} - \omega$ are the tracking errors. The control inputs are then:

$$V_{aR} = u_v + u_\omega \text{ and } V_{aL} = u_v - u_\omega$$

The gains, tuned manually to optimize simulation performance, are set as $K_{p_v} = 400$, $K_{i_v} = 300$, $K_{d_v} = 10$ for v, and $K_{p_\omega} = 20$, $K_{i_{\omega_z}} = 100$, $K_{d_\omega} = 0.5$ for ω. Discrete approximations are applied for the integral and derivative terms using a time step of $dt = 0.001$ s, with input saturation enforced at ± 48 V to reflect practical motor constraints.

2) LQR with Feedforward (LQR-ff)

The LQR-ff controller combines state feedback with a feedforward term to improve tracking, as described in [8]. The state feedback gain $\mathrm{K_{lqr}}$ is derived by minimizing the cost function $J = \int_0^\infty (\mathrm{x}^T \mathrm{Q_{lqr}} \mathrm{x} + \mathrm{u}^T \mathrm{R_{lqr}} \mathrm{u}) dt$, with $\mathrm{Q_{lqr}} = 0.2 \cdot \mathrm{diag}([1,1,1,1])$ and $\mathrm{R_{lqr}} = 300 \cdot \mathrm{I}_2$. These weights balance state regulation and control effort. The feedforward gain $\mathrm{K_{ff}} = -(\mathrm{CA}^{-1}\mathrm{B})^{-1}$ is calculated to eliminate steady-state error in the absence of disturbances by inverting the steady-state output mapping. The control law is $\mathrm{u} = -\mathrm{K_{lqr}} \mathrm{x} + \mathrm{K_{ff}} \mathrm{r}$, where x is the state vector and $\mathrm{r} = [v_{\text{ref}}, \omega_{\text{ref}}]^T$ is the reference. Control inputs are saturated at ± 48 V, consistent with system limits, and stability is ensured by verifying that all eigenvalues of $\mathrm{A} - \mathrm{BK_{lqr}}$ have negative real parts.

These controller designs provide a robust foundation for comparison with the proposed method, enabling an assessment of their performance in terms of disturbance rejection, tracking accuracy, and computational efficiency within the simulation environment.

C. Tracking Performance under Step Disturbances

Figure 7 illustrates how well v and ω align with their targets amid abrupt disturbances. Performance is evaluated using the Relative Root-Mean-Square Error (RRMSE) [30]. The developed system (pink dotted line) adheres closely to the intended path (gray solid line), yielding RRMSE scores of 9.2% for v and 8.5% for ω. In contrast, the PID controller (blue dashed line) struggles to track the reference, showing significant steady-state errors with RRMSE values of 13.4% for v and 39.2% for ω, particularly failing to correct deviations in ω. Meanwhile, the LQR-ff (red solid line) exhibits smaller but persistent deviations, with RRMSE values of 9.5% for v and 9.4% for ω, despite sudden force changes.

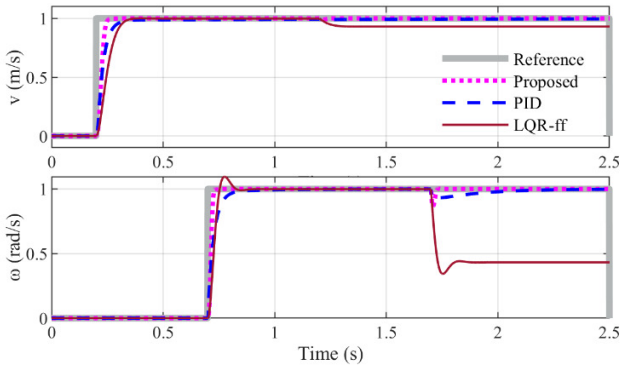

Fig. 7. Performance of v (m/s) and ω (rad/s) under step disturbances.

The control voltages V_{aR} and V_{aL} in Figure 8 reveal distinct controller behaviors under step disturbances and reference changes. The proposed controller (gray) demonstrates a smooth and rapid response, maintaining V_{aR} and V_{aL} within the saturation limit of ±48 V. This smooth behavior, driven by LQR optimization and integral action, ensures effective handling of disturbances and reference tracking while minimizing control effort. The PID controller (blue) exhibits significant oscillations, particularly during disturbance transitions and reference changes, leading to a chattering effect that can induce mechanical stress on the motors and increase energy consumption. The LQR-ff controller (red) shows smaller oscillations than the PID but fails to eliminate steady-state errors due to the absence of integral action. These findings highlight the controller's excellent capability to balance performance, stability, and energy efficiency, making it well-suited for practical DDWMR applications where step disturbances and dynamic reference changes are common.

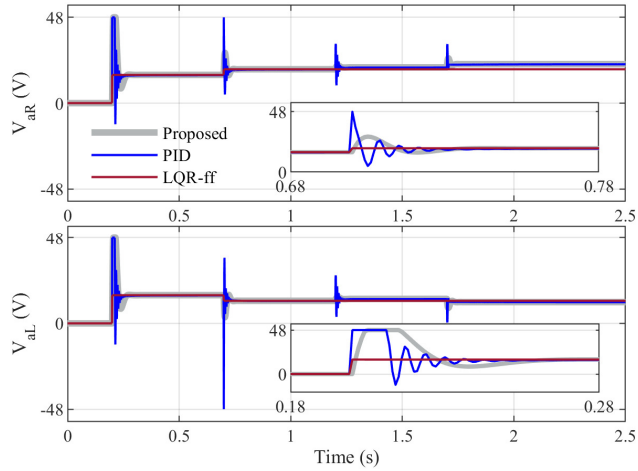

Fig. 8. Control voltages V_{aR} and V_{aL} (V) under step disturbances.

D. Tracking Performance under Random Disturbances

Under random Gaussian disturbances, the proposed controller demonstrates superior performance compared to the baselines (Figure 9), achieving RRMSE of 9.4% for v and 9.5% for ω that indicate robust tracking accuracy. In contrast, the PID controller yields higher RRMSE of 12.4% for v and 40.6% for ω, while the LQR-ff controller records 9.6% for v and 10.3% for ω. These larger errors highlight the limited robustness of both PID and LQR-ff to stochastic disturbances.

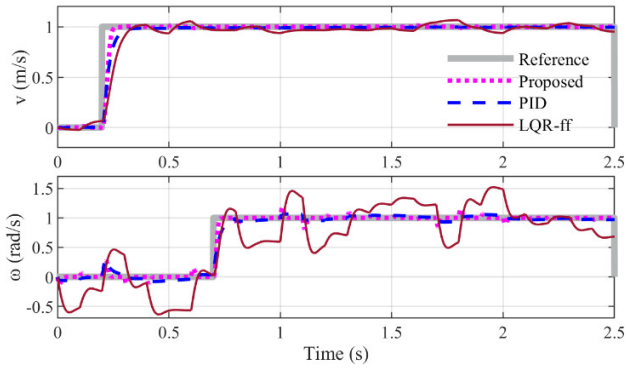

Fig. 9. Performance of v (m/s) and yaw rate ω (rad/s) under random Gaussian disturbances.

To analyze the controllers' responses to Gaussian disturbances, Figure 10 displays the control voltages V_{aR} and V_{aL} in the interval of 0.6 to 0.75 s for all three controllers: the proposed (gray), PID (blue dashed), and LQR-ff (red). During this period, the Gaussian noise changes rapidly, with a minimum segment width of 0.1 s, causing continuous fluctuations in the system states, particularly ω_R and ω_L. The PID controller exhibits pronounced high-frequency variations in its control signal, driven by the sensitivity of its proportional and derivative components to rapid noise-induced error changes. The LQR-ff controller, produces a nearly constant control signal, unable to respond effectively to the fast-changing noise due to its design, which lacks integral action, resulting in persistent steady-state errors. In contrast, the proposed controller delivers a significantly smoother control signal, leveraging the LQR optimization framework and an anti-windup mechanism to effectively manage integral error accumulation under noisy conditions.

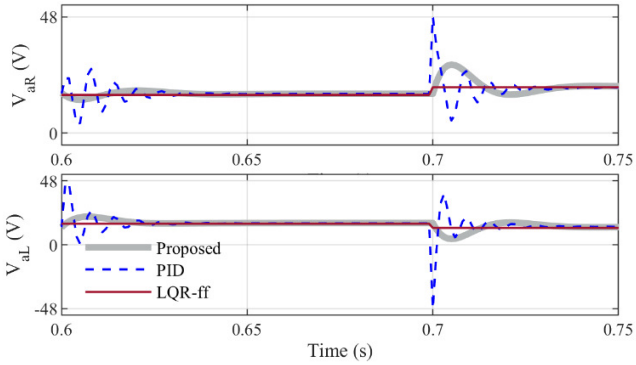

Fig. 10. Control voltages V_{aR} and V_{aL} (V) under Gaussian disturbances from 0.6 to 0.75 s.

These control signal characteristics have significant practical implications, as observed throughout the entire simulation duration (0- 2.5 s). High-frequency variations in the PID controller can lead to the chattering phenomenon, which

degrades tracking accuracy and imposes mechanical stress on the motors, potentially reducing their lifespan. The LQR-ff controller, while avoiding variations, sustains a nearly constant control signal that fails to adapt to disturbances, leading to steady-state offsets that compromise tracking precision. Meanwhile, the proposed controller consistently maintains a smooth response with minimal variations, demonstrating superior disturbance rejection and tracking performance. These findings highlight the effectiveness of the proposed approach in challenging operational scenarios, such as off-road navigation or automated warehousing, where random disturbances are common.

E. Comparative Analysis

Table I summarizes the RRMSE values for both disturbance scenarios. The proposed system reliably delivers the smallest RRMSE, showcasing strong path-following capability and robust disturbance rejection. Stability is further confirmed by the negative eigenvalues of the closed-loop system matrix A_{cl}. Its efficient design, which does not rely on disturbance observers, combined with its robust performance, renders it ideal for real-time use in DDWMRs in settings such as automated logistics and rugged terrain navigation.

TABLE I. PERFORMANCE COMPARISON UNDER STEP AND RANDOM DISTURBANCES ACROSS CONTROL METHODS

	Step disturbances		**Gaussian disturbances**	
Method	**RRMSE (v)**	**RRMSE (ω)**	**RRMSE (v)**	**RRMSE (ω)**
PID	13.4%	39.2%	12.4%	40.6%
LQR-ff	9.5%	9.4%	9.6%	10.3%
Proposed	9.2%	8.5%	9.4%	9.5%

V. CONCLUSION

This study introduced a robust MIMO LQR controller with integral action for DDWMRs to achieve precise trajectory tracking under external disturbances. By integrating integral action, the controller eliminates steady-state errors, while a novel Lyapunov-based analysis leveraging the LQR cost function ensures uniform ultimate boundedness. MATLAB simulations demonstrated RRMSE values below 10% for longitudinal speed and yaw rate, outperforming conventional PID and LQR-feedforward methods in both step and stochastic disturbance scenarios. Compared to complex methods such as MPC [12], the proposed approach offers a simpler and computationally efficient solution, ideal for resource-constrained real-time systems. The simulations utilized realistic physical parameters, such as wheel radius and base width, enhancing the applicability of the results. However, the method assumes bounded disturbances and fixed system parameters, which may limit performance under large or uncertain disturbances or varying conditions, such as payload changes, and experimental validation on physical DDWMR hardware remains pending. Future work will focus on real-world implementation, adaptive tuning to handle uncertain disturbances and parameter variations, and integration with higher-level path planning for enhanced autonomy.

REFERENCES

[1] R. Siegwart, I. R. Nourbakhsh, and D. Scaramuzza, *Introduction to Autonomous Mobile Robots*, 2nd ed. MIT Press, 2011.

[2] G. Campion, G. Bastin, and B. Dandrea-Novel, "Structural properties and classification of kinematic and dynamic models of wheeled mobile robots," *IEEE Transactions on Robotics and Automation*, vol. 12, no. 1, pp. 47–62, Oct. 1996, https://doi.org/10.1109/70.481750.

[3] W. He, Y. Chen, and Z. Yin, "Adaptive Neural Network Control of an Uncertain Robot With Full-State Constraints," *IEEE Transactions on Cybernetics*, vol. 46, no. 3, pp. 620–629, Mar. 2016, https://doi.org/10.1109/TCYB.2015.2411285.

[4] X. Gao, R. Gao, P. Liang, Q. Zhang, R. Deng, and W. Zhu, "A Hybrid Tracking Control Strategy for Nonholonomic Wheeled Mobile Robot Incorporating Deep Reinforcement Learning Approach," *IEEE Access*, vol. 9, pp. 15592–15602, 2021, https://doi.org/10.1109/ACCESS.2021.3053396.

[5] Z. Ge *et al.*, "Robust adaptive sliding mode control for path tracking of unmanned agricultural vehicles," *Computers and Electrical Engineering*, vol. 108, May 2023, Art. no. 108693, https://doi.org/10.1016/j.compeleceng.2023.108693.

[6] T. Yuan and R. Zhao, "LQR-MPC-Based Trajectory-Tracking Controller of Autonomous Vehicle Subject to Coupling Effects and Driving State Uncertainties," *Sensors*, vol. 22, no. 15, Jan. 2022, Art. no. 5556, https://doi.org/10.3390/s22155556.

[7] K. J. Astrom and T. Hagglund, *PID Controllers: Theory, Design and Tuning*. ISA, 1995.

[8] B. D. O. Anderson and J. B. Moore, *Optimal Control: Linear Quadratic Methods*. Dover Publications, 2007.

[9] H. Ye and S. Wang, "Trajectory Tracking Control for Nonholonomic Wheeled Mobile Robots with External Disturbances and Parameter Uncertainties," *International Journal of Control, Automation and Systems*, vol. 18, no. 12, pp. 3015–3022, Dec. 2020, https://doi.org/10.1007/s12555-019-0643-y.

[10] H. Huang, J. Zhou, Q. Di, J. Zhou, and J. Li, "Robust neural network–based tracking control and stabilization of a wheeled mobile robot with input saturation," *International Journal of Robust and Nonlinear Control*, vol. 29, no. 2, pp. 375–392, 2019, https://doi.org/10.1002/rnc.4396.

[11] Y. Cao, K. Ni, T. Kawaguchi, and S. Hashimoto, "Path Following for Autonomous Mobile Robots with Deep Reinforcement Learning," *Sensors*, vol. 24, no. 2, Jan. 2024, Art. no. 561, https://doi.org/10.3390/s24020561.

[12] E. F. Camacho and C. B. Alba, *Model Predictive Control*. Springer, 2013.

[13] Z. Sun, R. Wang, X. Meng, Y. Yang, Z. Wei, and Q. Ye, "A novel path tracking system for autonomous vehicle based on model predictive control," *Journal of Mechanical Science and Technology*, vol. 38, no. 1, pp. 365–378, Jan. 2024, https://doi.org/10.1007/s12206-023-1230-y.

[14] J. Peng, H. Xiao, and G. Lai, "Nonlinear Disturbance Observer Incorporated Model Predictive Strategy for Wheeled Mobile Robot's Trajectory Tracking Control," *International Journal of Control, Automation and Systems*, vol. 22, no. 7, pp. 2251–2262, Jul. 2024, https://doi.org/10.1007/s12555-023-0207-z.

[15] V. Utkin, J. Guldner, and J. Shi, *Sliding Mode Control in Electro-Mechanical Systems*, 2nd ed. CRC Press, 2017.

[16] X. Ji, X. Wei, A. Wang, B. Cui, and Q. Song, "A novel composite adaptive terminal sliding mode controller for farm vehicles lateral path tracking control," *Nonlinear Dynamics*, vol. 110, no. 3, pp. 2415–2428, Nov. 2022, https://doi.org/10.1007/s11071-022-07730-x.

[17] S. L. Dai, S. He, X. Chen, and X. Jin, "Adaptive Leader–Follower Formation Control of Nonholonomic Mobile Robots With Prescribed Transient and Steady-State Performance," *IEEE Transactions on Industrial Informatics*, vol. 16, no. 6, pp. 3662–3671, Jun. 2020, https://doi.org/10.1109/TII.2019.2939263.

[18] H. Medjoubi, A. Yassine, and H. Abdelouahab, "Design and Study of an Adaptive Fuzzy Logic-Based Controller for Wheeled Mobile Robots Implemented in the Leader-Follower Formation Approach,"

Engineering, Technology & Applied Science Research, vol. 11, no. 2, pp. 6935–6942, Apr. 2021, https://doi.org/10.48084/etasr.3950.

[19] J. Doyle, "Robust and optimal control," in *Proceedings of 35th IEEE Conference on Decision and Control*, Kobe, Japan, 1996, vol. 2, pp. 1595–1598, https://doi.org/10.1109/CDC.1996.572756.

[20] C. C. Tsui, "High-performance state feedback, robust, and output feedback stabilizing control-a systematic design algorithm," *IEEE Transactions on Automatic Control*, vol. 44, no. 3, pp. 560–563, Mar. 1999, https://doi.org/10.1109/9.751350.

[21] M. Saeedi, J. Zarei, M. Saif, and A. Montazeri, "Event-Based Robust Control Techniques for Wheel-Based Robots Under Cyber-Attack and Dynamic Quantizer," in *Mobile Robot: Motion Control and Path Planning*, A. T. Azar, I. Kasim Ibraheem, and A. Jaleel Humaidi, Eds. Springer International Publishing, 2023, pp. 163–196.

[22] Y. Wang, Z. Miao, H. Zhong, and Q. Pan, "Simultaneous Stabilization and Tracking of Nonholonomic Mobile Robots: A Lyapunov-Based Approach," *IEEE Transactions on Control Systems Technology*, vol. 23, no. 4, pp. 1440–1450, Jul. 2015, https://doi.org/10.1109/TCST.2014.2375812.

[23] C. Liu, J. Gao, and D. Xu, "Lyapunov-based model predictive control for tracking of nonholonomic mobile robots under input constraints," *International Journal of Control, Automation and Systems*, vol. 15, no. 5, pp. 2313–2319, Oct. 2017, https://doi.org/10.1007/s12555-016-0350-x.

[24] M. Chen, "Robust tracking control for self-balancing mobile robots using disturbance observer," *IEEE/CAA Journal of Automatica Sinica*, vol. 4, no. 3, pp. 458–465, 2017, https://doi.org/10.1109/JAS.2017.7510544.

[25] M. Fouzia, N. Khenfer, and N. E. Boukezzoula, "Robust Adaptive Tracking Control of Manipulator Arms with Fuzzy Neural Networks," *Engineering, Technology & Applied Science Research*, vol. 10, no. 4, pp. 6131–6141, Aug. 2020, https://doi.org/10.48084/etasr.3648.

[26] N. T. T. Vu, N. P. Tran, and N. H. Nguyen, "Recurrent Neural Network-based Path Planning for an Excavator Arm under Varying Environment," *Engineering, Technology & Applied Science Research*, vol. 11, no. 3, pp. 7088–7093, Jun. 2021, https://doi.org/10.48084/etasr.4125.

[27] A. M. D. Tran, T. V. Vu, and Q. D. Nguyen, "A Study on General State Model of Differential Drive Wheeled Mobile Robots," *Journal of Advanced Engineering and Computation*, vol. 7, no. 3, Sep. 2023, Art. no. 174, https://doi.org/10.55579/jaec.202373.417.

[28] H. Khalil, *Nonlinear Systems*. Upper Saddle River, NJ, USA: Pearson, 2002.

[29] R. Fareh, M. R. Saad, M. Saad, A. Brahmi, and M. Bettayeb, "Trajectory Tracking and Stability Analysis for Mobile Manipulators Based on Decentralized Control," *Robotica*, vol. 37, no. 10, pp. 1732–1749, Oct. 2019, https://doi.org/10.1017/S0263574719000225.

[30] A. M. D. Tran and T. V. Vu, "A Dynamic Controller Architecture for Wheeled Mobile Robot Trajectory Tracking Utilizing Feedback Linearization and State Feedback," *Journal of Advanced Engineering and Computation*, vol. 8, no. 2, pp. 119–129, Jun. 2024, https://doi.org/10.55579/jaec.202482.456.